Biosensors and Bioelectronics 143 (2019) 111608

Contents lists available at ScienceDirect

Biosensors and Bioelectronics

journal homepage: www.elsevier.com/locate/bios

Novel electrochemical immunosensor for sensitive monitoring of cardiac troponin I using antigen–response cargo released from mesoporous Fe_3O_4

Ning Ma, Tong Zhang, Tao Yan, Xuan Kuang, Huan Wang, Dan Wu*, Qin Wei

Key Laboratory of Interfacial Reaction & Sensing Analysis in Universities of Shandong, University of Jinan, Jinan, 250022, PR China

ARTICLE INFO

Keywords:
Mesoporous Fe_3O_4
Controlled release
Cardiac troponin I
Amperometric i-t detection method

ABSTRACT

A novel controlled release system-based antigen-response electrochemical immunosensor was developed for detecting cardiac troponin I (cTnI) by using aminated polystyrene microsphere (APSM) as molecular gate and Fe_3O_4 as nanocontainer. The amino functionalized mesoporous Fe_3O_4 (Fe_3O_4–NH_2) was used to load cobalt phthalocyanine nanoparticles (CoPc NPs) and further capture the antibody of cTnI (Ab) to form Fe_3O_4-Ab. In addition, APSM was introduced to cap on the mesoporous of Fe_3O_4-Ab by electrostatic interaction. With the addition of cTnI, APSM was separated from Fe_3O_4-Ab due to the specific binding of antibody to antigen. Then, CoPc NPs were released from the mesoporous. The experimental results revealed that CoPc NPs showed superb catalytic performance when catalyzing hydrogen peroxide (H_2O_2) reduction in phosphate buffer saline (PBS). The current responses are correlated with the amount of cTnI. Under the best conditions, a broad linear range from 1.0 pg/mL to 100 ng/mL with a low detection limit of 0.39 pg/mL (S/N = 3) was obtained. The immunosensor also shows good reproducibility and selectivity, which endows its broad application prospect in clinical research.

1. Introduction

Coronary heart disease caused by coronary artery occlusion is one of the most dangerous diseases to human health. Complications such as acute myocardial infarction (AMI), angina pectoris, or heart failure arise from interruption of myocardial blood supply are enough to threaten people's lives (Jain et al., 1995a; Srivastava et al., 1996; Zheng et al., 2016). As a regulatory protein for myocardial muscle contraction, cardiac troponin (cTn) consists of I subtype (cTnI), T subtype, and C subtype (Gupta and Kumar 1999; Gupta et al., 2013; Nandhikonda and Heagy, 2011). When AMI occurs, cTnI can be specifically released into the blood for a short time without being affected by other troponin subtypes in skeletal muscle. Therefore, cTnI, as a specific biomarker, plays an important role in the detection and treatment of acute coronary syndrome (Gupta et al., 2011; Wang et al., 2019). It is of great significance to detect cTnI quickly and accurately (Liu et al., 2016; Sarangadharan et al., 2018; Srivastava et al., 1995). There are various methods for detecting cTnI including colorimetric, fluorescence, paramagnetic and surface plasmon resonance (Cho et al., 2009; Masson et al., 2004; Srivastava et al., 1995).

In recent years, the research on controlled release of small molecules from mesoporous material has received special attention (Gupta et al., 2012; Jain et al., 1995b; Liu et al., 2015). Its timing release characteristics can be used in drug release research. Furthermore, controlled release technology also can be used for accurate and convenient quantitative detection of biomolecules with rapid detection methods (Gao et al., 2015; Gupta et al., 2014c; Karthikeyan et al., 2012). Many kinds of release mechanisms have been widely discussed. The most common way to realize controlled release is controlling the physical blockages to leave the mesoporous of porous materials (Asfaram et al., 2015; Dehghani et al., 2016; Liu et al., 2010). However, the controlled release system for substance detection often requires convenient and rapid detection methods. Therefore, the combination of controlled release and electrochemical detection can realize the rapid detection of cTnI.

For the nanocontainer of controlled release system, porous materials have attracted special interest of scientists in this field, which can accommodate small molecular markers from reaction environment not only because of their large specific surfaces area but also because of their channel characteristics (Gupta et al., 2014b; Yola et al., 2014; Zhang et al., 2018a). Various types of porous materials including mesoporous ferric oxide (Fe_3O_4) nanospheres, covalent organic frameworks (COFs), conjugated microporous polymers (CMPs) and metal-organic frameworks (MOFs) have emerged (Gu et al., 2010; Liao et al., 2017; Schulze et al., 2015; Wan et al., 2013; Wang et al., 2017; Zou et al., 2017). With the advantages of high biocompatibility, non-toxic

* Corresponding author.
E-mail address: wudan791108@163.com (D. Wu).

https://doi.org/10.1016/j.bios.2019.111608
Received 11 June 2019; Received in revised form 11 August 2019; Accepted 17 August 2019
Available online 17 August 2019
0956-5663/

metal constituent and low toxicity, Fe_3O_4 nanospheres have been widely used in the field of biological detection. These particles also have the advantage of magnetic separation in the process of making and using due to its magnetism (Gupta et al. 2014a, 2015a; Xuan et al., 2011). In this way, Fe_3O_4 nanospheres can be directly modified on the magnetic electrode, thereby reducing the modification steps and experimental errors. Therefore, Fe_3O_4 nanospheres were used as the nanocontainer for this immunosensor.

As an important part of the controlled release system, it is necessary to choose the suitable cargo that can be released sensitively and accurately. Cobalt phthalocyanine (CoPc), with a Co (II)/Co (I) redox couple and excellent electrocatalytic activity towards hydrogen peroxide (H_2O_2), ascorbic acid and bisphenol A, has drawn extensive concern in the field of immunosensor (Gupta et al., 2015b; Li et al., 2014; Zhu et al., 2018). Unfortunately, owing to the large-conjugated systems, CoPc has the limitations of hydrophobicity and aggregation, which blocks the wide-spread application of CoPc. To overcome the drawbacks, $C_{16}H_{33}N(CH_3)_3Br$ (CTAB) was introduced as a surfactant to enhance the hydrophilicity and dispersion. Furthermore, the redox activity of CoPc nanoparticles (CoPc NPs) was also significantly increased (Zhu et al., 2018). In addition, the size of CoPc NPs also fits into the mesoporous structure of Fe_3O_4 nanospheres. Therefore, already well dispersed CoPc NPs were prepared as the cargo of immunosensor.

Herein, a controlled release system-based analytical device was employed for electrochemical detection of cTnI by aminated polystyrene microsphere (APSM) gated Fe_3O_4. The glutaraldehyde was selected as coupling agents to connect antibodies (Ab) and amine-functionalized mesoporous Fe_3O_4 (Fe_3O_4–NH_2). Then, with the right size to fit the pore diameter of Fe_3O_4, CoPc NPs were loaded into the mesoporous of Fe_3O_4, and APSM blocked the mesoporous through the electrostatic interaction between Fe_3O_4–NH_2 and APSM. As the core step of immunosensor, after the addition of cTnI, the trapped CoPc NPs were released from the mesoporous because APSM was replaced by cTnI through antigen-antibody bind and left from the surface of Fe_3O_4-Ab. Then, CoPc NPs were released from the mesoporous. The released CoPc NPs showed superb catalytic performance when catalyzing H_2O_2 reduction in phosphate buffer saline (PBS). The current responses are correlated with the amount of cTnI. The resulted immunosensor displayed good specificity and high sensitivity, implying potential applications in clinical analysis.

2. Experimental section

2.1. Reagents

cTnI antigen and antibody were bought from Shanghai Linc-Bio Science Co., Ltd., China. Other details are displayed in the supplementary material.

2.2. Apparatus

All electrochemical experiments were performed on CHI760E electrochemical workstation, which was manufactured from this company of Shanghai CH Instruments Co, China. Details of other instruments will be described in the supplementary material.

2.3. Preparation of the Fe_3O_4–NH_2

Scheme 1Aexhibited the construction process of the controlled release immunosensor. A one-step solvothermal method was employed for the synthesis of Fe_3O_4–NH_2. In a typical synthesis procedure (Karunakaran et al., 2018; Pan et al., 2018), iron chloride anhydrous ($FeCl_3$) (2 g) were added into ethylene glycol (40.0 mL) and dissolving to obtain a clear and transparent solution. After that, anhydrous sodium acetate (6 g) and ethylenediamine (20 mL) were put into the solution and vigorously stirred vigorously for 30 min. As the following step, the mixed solution was poured into reaction still and heated in the oven to 200 °C for 8 h. The rate of warming or cooling was disregarded in the reaction. After cooling to normal temperature, the precipitate in vessel was washed with plenty of ultrapure water and magnetically separated. When the supernatant was neutral, the washing was stopped, and the resulting precipitate was dried in an oven at 50 °C.

2.4. Preparation of Fe_3O_4-Ab

Fe_3O_4-Ab was synthesized on the grounds of disclosed synthesis methods with revisions (Zhang et al., 2013). Firstly, 50 mg Fe_3O_4–NH_2 was dispersed in ethanol (1 mL) by ultrasonic. Then, 300 μL glutaraldehyde (25 wt%) was added into the mixed solution and the solution was stirred at normal temperature for 6 h. Next, the sediment was washed three times with ultrapure water and the synthesized modified Fe_3O_4 was obtained by magnetic separation. After that, the modified Fe_3O_4 was dissolved in PBS (300 μL, pH = 7.6) including Ab (0.2 mg/mL), and incubated for 6 h at 4 °C. In order to block the active sites remain on the surface of Fe_3O_4, 10 μL bovine serum albumin (BSA) (10 wt%) was added into the solution. After that, the mixed solution was incubated for 2 h at 4 °C. To reduce the resultant Schiff bases or any excess aldehydes in mixed solution, sodium borohydride solution (50 μL, 25 mg/mL) was added. After incubated at 4 °C for 1 h, the suspension was separated by the magnet and the magnetic Fe_3O_4-Ab was stored at 4 °C in PBS (1.0 mL, pH = 7.6).

2.5. Loading CoPc NPs in Fe_3O_4-Ab

Loading of CoPc NPs in Fe_3O_4-Ab was accomplished by the following procedure (Zhang et al., 2013). First, 60 mg of CoPc NPs was added into 1 mL PBS containing Fe_3O_4-Ab (10 mg/mL) and shaken for 6 h at 4 °C. In this process, numerous CoPc NPs were dispersed in the mesoporous of Fe_3O_4. Then the loaded Fe_3O_4-Ab was separated by the magnet and dispersed in PBS containing APSM (25 mg/mL) immediately. As a kind of positively charged microspheres, APSM can cover the mesoporous of negative charged Fe_3O_4-Ab by electrostatic adsorption. After incubated in thermostat incubator at 4 °C for 6 h, the mixture was washed with PBS (pH = 7.6) for several times until a low current response was exhibited. The obtained APSM-capped CoPc NPs-Fe_3O_4-Ab (Fe_3O_4@APSM) was maintained in PBS (1.0 mL, pH = 7.6) for further usage.

2.6. Fabrication of the immunosensor

In general, the magnetic glassy carbon electrode (MGCE) was polished regularly to a smooth surface by alumina powder with 1.0, 0.5 and 0.05 μm alumina powder ordinal and washed by ultrapure water. Next, Fe_3O_4@APSM solution (10 μg/mL, 8.0 μL) was modified to the surface of the MGCE through magnetism. After washed by purified water, the resulting MGCE was covered by cTnI (1 wt%, 3 μL) to release CoPc NPs. After 25 min, the MGCE was put into the PBS solution for further detection.

2.7. Detection of cTnI

All electrochemical measurements of this system were based on conventional three-electrode system: A modified MGCE (6 mm in diameter) as the working electrode, a saturated calomel electrode (SCE) as the reference electrode and a platinum wire as the counter electrode. The PBS (pH = 7.6) was used as electrolyte solution. The released CoPc NPs can catalyze the added H_2O_2 to detect cTnI. It was due to the added H_2O_2 oxidizes the cobalt element in CoPc NPs from Co (I) to Co (II) (Scheme 1B) (Yang et al., 2016). For amperometric measurement of the immunosensor, −0.4 V was selected as detection potential because such a low potential would be beneficial to decrease the background

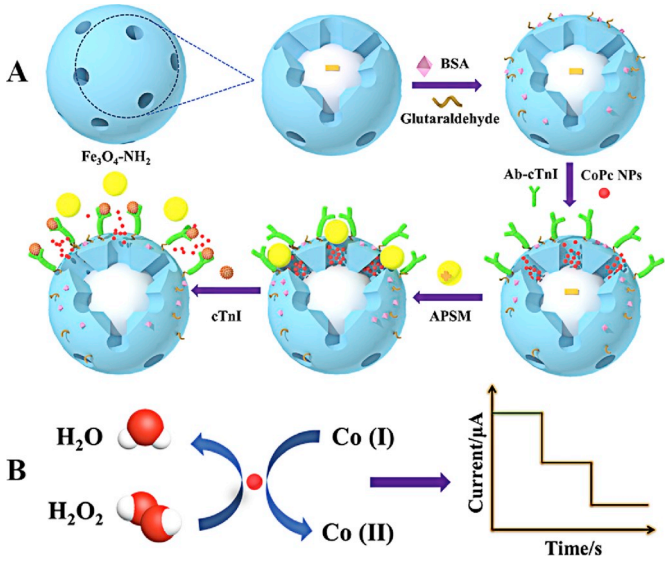

Scheme 1. The preparation procedure of the sandwich-type electrochemical immunosensor.

current and minimize the responses of common interference species. After the background current was stabilized, H_2O_2 (4 mol/L, 10 μL) was added to the buffer solution, and the current change was recorded. All the experiments were carried out at room temperature.

3. Results and discussion

3.1. Characterization of the nanocomposites

As depicted in Fig. 1A, CoPc NPs had a uniform size of 8–10 nm in diameter in scanning electron microscope (SEM) image. The transmission electron microscope (TEM) diagram in Fig. 1B further showed that CoPc NPs had good dispersion. The diameter of Fe_3O_4–NH_2 was characterized by TEM. As was illustrated in Fig. 1C, with a mean diameter of 150 nm, Fe_3O_4–NH_2 had abundant of mesoporous with a size ranging from 20 to 25 nm, indicating the spherical CoPc NPs can easily enter the mesoporous structure of Fe_3O_4.

The composition of Fe_3O_4 could be further certified by X-ray power diffraction (XRD). The curve of Fig. 2A matched well with the diffraction peaks of Fe_3O_4 (JCPDS card no. 26–1136). It also suggested that Fe_3O_4 nanohybrid was synthesized successfully. In the range of 4000–400 cm^{-1}, the Fourier transform infrared (FT-IR) of Fe_3O_4–NH_2 was shown in Fig. 2B. In-plane deforming vibrations and stretching vibrations of N–H bond produce the absorption peaks of 1630 cm^{-1} and 3430 cm^{-1}, respectively. From this, it can be seen that Fe_3O_4–NH_2 were successfully synthesized. As shown in Fig. 2C, the nitrogen sorption technique was used to characterize the porosity analyzer and specific surface area of Fe_3O_4–NH_2. The pore size was centered at 20 nm from the pore size distribution curve of Fe_3O_4. H3 hysteresis loop and IV type isotherm were shown in the inset of Fig. 2C, which indicated the existence of mesoporous on the surface of Fe_3O_4–NH_2. In the test of Brunauer-Emmett-Teller (BET), surface area and mesoporous volumes were 73.134 m^2/g and 0.318 cm^3/g, respectively. From the Zeta

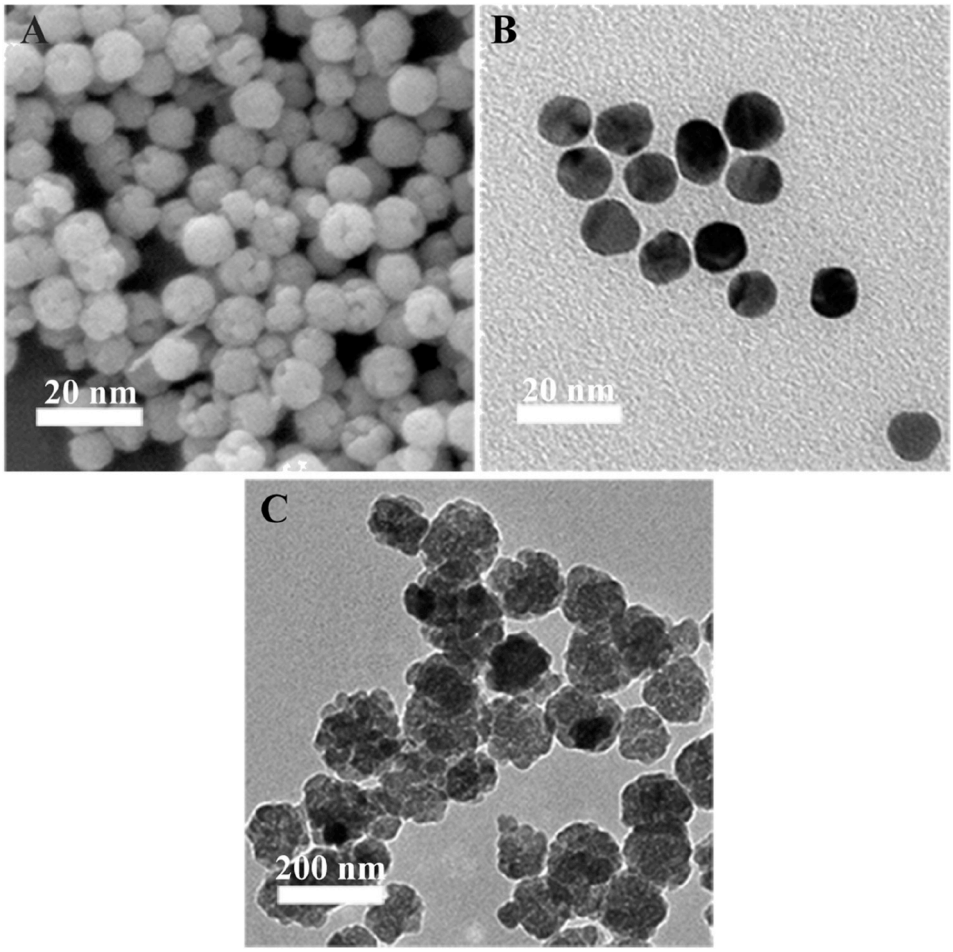

Fig. 1. (A) The SEM image of nanoCoPc; The TEM image of (B) nanoCoPc and (C) Fe_3O_4–NH_2.

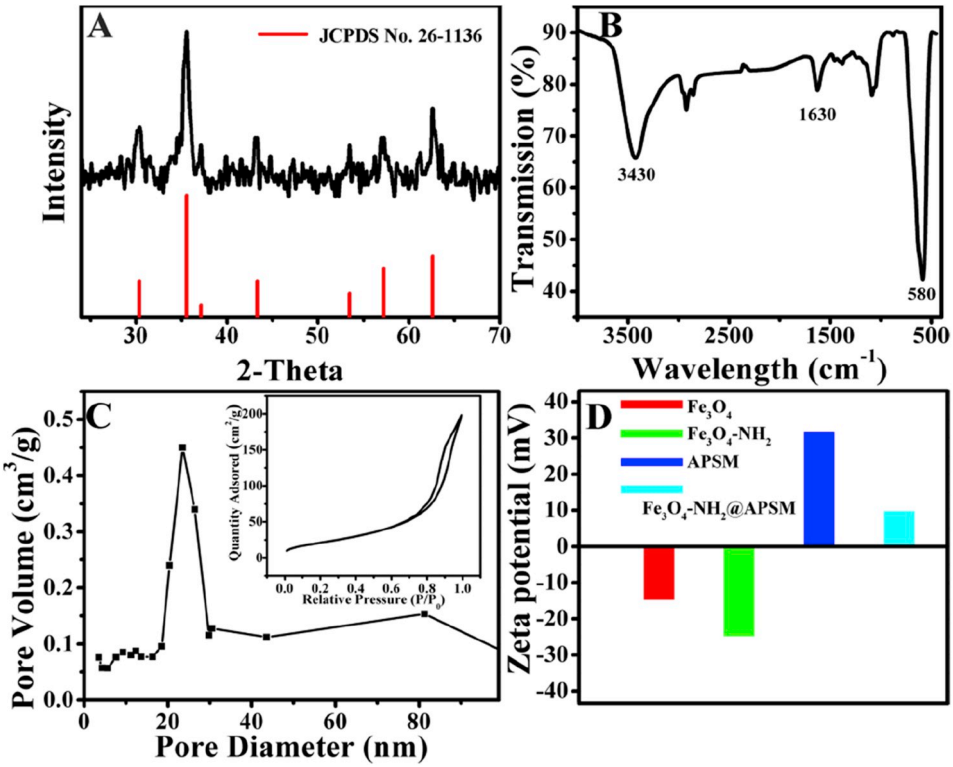

Fig. 2. (A) The XRD image of Fe_3O_4; (B) The FT-IR of Fe_3O_4–NH_2; (C) The pore size distribution of Fe_3O_4, the inset is nitrogen adsorption-desorption isotherm of Fe_3O_4 and (D) Zeta potentials of Fe_3O_4, Fe_3O_4–NH_2, APSM and Fe_3O_4–NH_2@APSM.

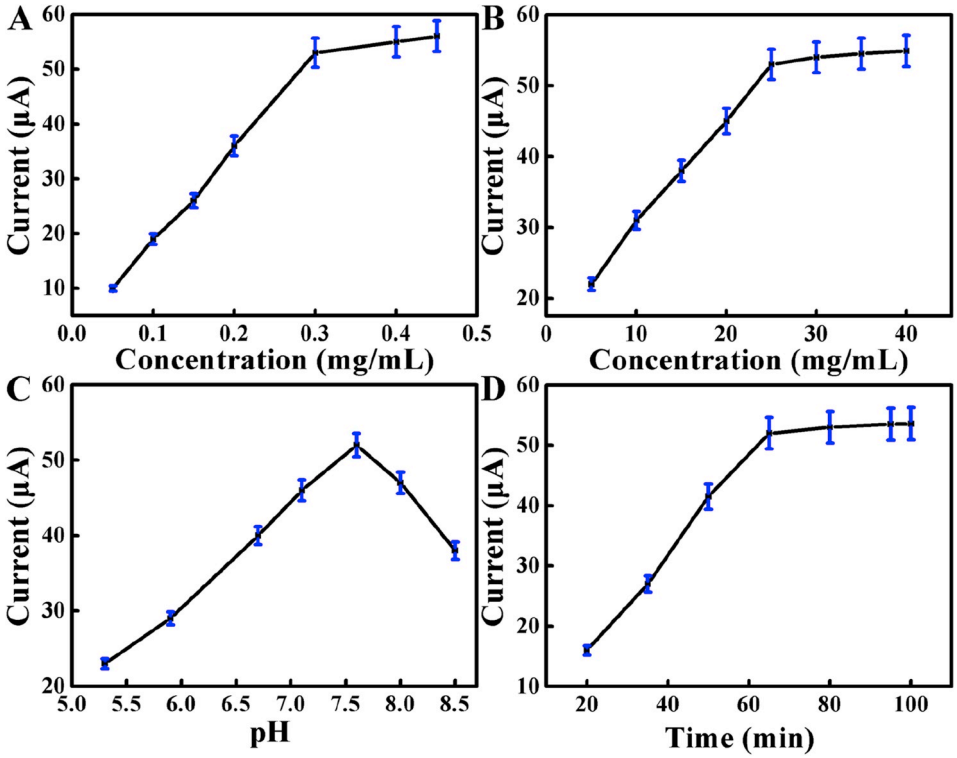

Fig. 3. The optimization of experimental conditions with (A) Ab concentration, (B) APSM concentration, (C) pH and (D) release time.

potentials (Fig. 2D), there was an electrostatic interaction between Fe_3O_4–NH_2 and APSM. The potential of Fe_3O_4–NH_2@ APSM was less than APSM, indicating the successful combination of Fe_3O_4–NH_2 and APSM.

3.2. Optimization of experimental conditions

In order to make the immunosensor achieve the most sensitive state to detect cTnI, the experimental conditions were optimized. First, during the construction of the controlled release system, Ab acted as a

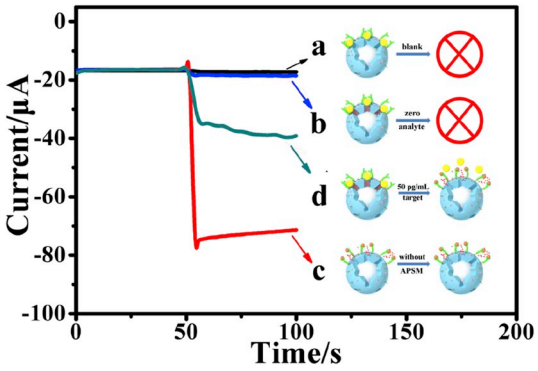

Fig. 4. Study of the entrapping capacity of Fe_3O_4 toward cargo (CoPc NPs) molecules into the mesoporous nanocontainer by the APSM; (a) Ab-Fe_3O_4 loading without CoPc NPs in the blank PBS, (b) Ab-Fe_3O_4 loading with CoPc NPs toward the zero analyte, (c) Ab-Fe_3O_4 loading CoPc NPs without APSM, and (d) Ab-Fe_3O_4 loading with CoPc NPs in the presence of 50 pg/mL. Incubation time: 65 min.

role of the gate frame which determines whether the molecular void can be blocked. Hence, the concentration of Ab in the experiment had a significant effect on the response current in the experimental results. Therefore, Ab in the range of 0.05–0.5 mg/mL was selected as the test object. As shown in Fig. 3A, as the concentration of Ab increases, the current response increases rapidly. When the concentration of cTnI was above 0.3 mg/mL, cTnI was saturated at the surface of Fe_3O_4–NH_2, the signal tends to stabilize. Therefore, 0.3 mg/mL was selected for the detection of cTnI.

APSM and Fe_3O_4–NH_2 nanoparticles were connected by electrostatic force, therefore the concentration of APSM played an important role in the construction of immunosensor. APSM acted as a molecular gate to block the Fe_3O_4 mesoporous, thus enabling the encapsulation of CoPc NPs. The APSM solution at a concentration of 5–40 mg/mL was then used to study the change in the current response. As shown in Fig. 3B, as the concentration of APSM increases, more and more mesoporous can be blocked by APSM and the current response increases. When the concentration of APSM was higher than 25 mg/mL, the amount of APSM on the surface of Fe_3O_4 was saturated, and the current response value tended to be stable. Therefore, the concentration of 25 mg/mL was chosen as the experimental concentration of APSM.

pH was also an essential conditional selection indicator. First, the electrochemical response properties of CoPc NPs in solution change with pH. In addition, the biological activities of cTnI and Ab were also related to the pH of the solution, and the excessively acidic or over-based environment affects the specific binding of antigen-antibody. Following that, a series of PBS with pH 5.3–8.5 were selected as experimental conditions. It can be seen from Fig. 3C that the current response increases from pH 5.3 to 7.6, and the current response declined between pH 7.6 and 8.5. It can be seen that cTnI bind effectively to Ab at pH = 7.6, achieving the best sealing effect. So this pH = 7.6 was selected as the pH value for the experiment.

As a controlled release system, whether encapsulated cargo can be quickly and stably released was also an aspect that needed to be studied. The 20–100 min was selected as the interval to be studied. It can be seen from the Fig. 3D that the current response was almost unchanged after 65 min of release, and the closed CoPc NPs was completely released. Therefore, 65 min was selected as the release time.

3.3. The mechanism of entrapping capacity

Under the best experimental conditions, a series of controlled experiments were tested by using the synthesized Fe_3O_4-Ab and APSM (Fig. 4). The capping efficiency of Fe_3O_4-Ab toward CoPc NPs by APSM was examined as following. Firstly, after blocking the mesoporous of Fe_3O_4-Ab by APSM without any CoPc NPs controlled, the current response displayed blank values on curve a. When the target cTnI was not added to release the CoPc NPs, the current response (curve b) was almost zero, indicating no leakage of CoPc NPs. However, without the cover of positively charged APSM, the current response enhanced obviously (curve c). The result revealed that APSM was effective for encapsulating CoPc NPs into Fe_3O_4-Ab. For further study, the 50 pg/mL cTnI was added into solution for controlled release detection. As shown in curve d, the current response was also bigger than those of curve a and b, indicating the cTnI was combined with Ab, and APSM moved away from the surfaces of Fe_3O_4. Thus, encapsulated CoPc NPs were released from the pores (Hou et al., 2014). The resultant suggested that the signal of immunosensor was corresponding to the concentration of target cTnI.

3.4. Analysis and detection of cTnI

After different concentrations of cTnI were modified on the electrodes, the i-t current response values were recorded in Fig. 5A. The linear relationship of the proposed immunosensor between the peak current and the concentration of cTnI was obtained in the range of 1.0 pg/mL-100 ng/mL (Fig. 5B), and the equation was ΔI (μA) = 12.12 lgc (pg/mL) + 16.75 (R = 0.9926). As we know, the limit of detection (LOD), expressed as the concentration, was derived from the smallest measure signal that can be detected with reasonable certainty for a given analytical procedure (Ren et al., 2015). In this study, the LOD of 0.39 pg/mL was calculated based on the signal-to-noise ratio (S/N = 3). The linear performance of our immunosensor was comparable or even better than those of previous reports for cTnI detection, the results were illustrated in Table S1. Because of the two main factors, the sensitivity and stability of the proposed immunosensor were significantly improved. For the first, as the nanocontainer of CoPc NPs, Fe_3O_4@APSM

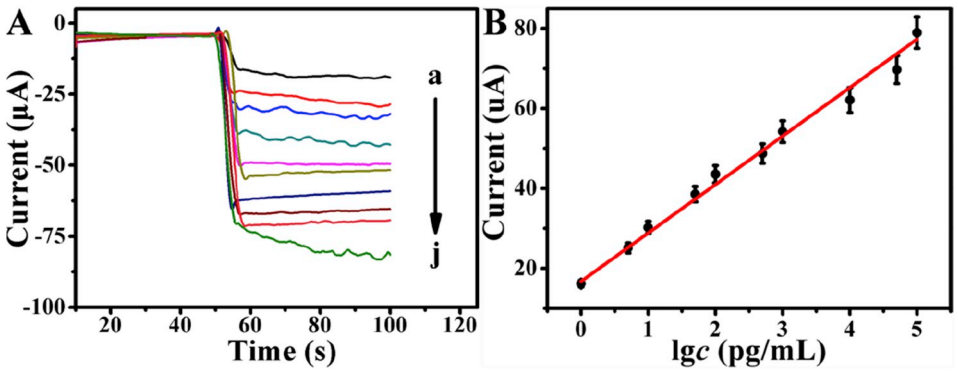

Fig. 5. (A) Amperometric responses of different modified electrodes in pH 7.6 PBS: (a) 1 pg/mL, (b) 5 pg/mL, (c) 10 pg/mL, (d) 50 pg/mL, (e) 0.1 ng/mL, (f) 0.5 ng/mL, (g) 1 ng/mL, (h) 10 ng/mL, (i) 50 ng/mL and (j) 100 ng/mL; (B) Calibration curves of immunosensor to different concentrations of cTnI, error bar = RSD (n = 5).

can encapsulate cargo inside the mesoporous steadily until cTnI replaces APSM by the antigen-antibody binding. What's more, the tested CoPc NPs revealed great catalytic characteristic, which could intensively promote the degree of H_2O_2 reduction. Therefore, high sensitivity becomes a highlight of this immunosensor.

3.5. Reproducibility and selectivity

Good reproducibility and stability were essential for the protocol (Zhang et al. 2018b, 2018c). As shown in Fig. S2A, stable current response curves with cTnI have been expressed. cTnI (1 ng/mL) was detected on five different electrodes. The relative standard deviation (RSD) of the measurements could be controlled to be 1.74%, including that the reproducibility and precision of the proposed platform were satisfactory.

To investigate the specificity of the proposed immunosensor, interferences study was performed by using squamous cell carcinoma antigen (SCCA), immunoglobulin G (IgG), carcino-embryonic antigen (CEA), BSA, Na^{2+} and Mg^{2+} (Ren et al. 2017a, 2017b). As shown in Fig. S2B, the data (1–7) showed that the current response values of the immunosensor with various interfering antigen and metal ions were less than 5% compared with the primary one. When 3 μL of interfering substance were added to the surface of electrode respectively without cTnI (data 8–13), there was no obvious current response, indicating that the selectivity of the controlled release system was satisfactory.

3.6. Real sample analysis

To monitor the possible application of the developed immunosensor for real samples, various concentrations of cTnI were added into human serum through the standard addition method. As shown in Table S2, the satisfactory RSD (0.52–0.90%) and recovery results (96.7–98.9%) suggested that the prepared immunosensors would be competent for directly determining the cTnI in serum samples. Furthermore, enzyme linked immunosorbent assay (ELISA) method was used as a reference method to validate the proposed method. By using ELISA method and the proposed methods, cTnI was determined 5 times, respectively. The results are shown in Table S3. The relative error between the two methods was - 0.40%. Hence, the accuracy of this method was acceptable and the feasibility of application in human serum is verified.

4. Conclusion

In this work, we have successfully synthesized Fe_3O_4–NH_2 with suitable mesoporous size to encapsulate CoPc NPs for cTnI detection. The released CoPc NPs can catalyze the added H_2O_2 to detect cTnI by amperometric i-t detection method. Compared with conventional electrochemical assay protocols, this system is inexpensive and easy to fix without the need for the connection of the base material. In addition, the developed immunosensor exhibits a broad relatively linear range, low detection limit and sensitivity for cTnI detection, providing a promising way for the determination of cTnI in clinical applications. Furthermore, this system may also be widely applied in the detection on environmental monitoring, food safety and clinical medical application.

Conflict of interest

Here I confirm there are no potential conflicts of interest.

Declaration of competing interest

The authors declare that they have no known competing financial interests or personal relationships that could have appeared to influence the work reported in this paper.

Acknowledgments

We gratefully acknowledge the financial support of the National Natural Science Foundation of China (Grant no. 21775054), the Natural Science Foundation of Shandong Province (Grant no. ZR2016JL013). All of the authors express their sincere thanks.

Appendix A. Supplementary data

Supplementary data to this article can be found online at https://doi.org/10.1016/j.bios.2019.111608.

References

Asfaram, A., Ghaedi, M., Agarwal, S., Tyagi, I., Kumar Gupta, V., 2015. RSC Adv. 5, 18438–18450.
Cho, I.-H., Paek, E.-H., Kim, Y.-K., Kim, J.-H., Paek, S.-H., 2009. Anal. Chim. Acta 632, 247–255.
Dehghani, M.H., Sanaei, D., Ali, I., Bhatnagar, A., 2016. J. Mol. Liq. 215, 671–679.
Gao, J., Guo, Z., Yu, S., Su, F., Ma, H., Du, B., Wei, Q., Pang, X., 2015. Biosens. Bioelectron. 66, 141–145.
Gu, Z.-Y., Wang, G., Yan, X.-P., 2010. Anal. Chem. 82, 1365–1370.
Gupta, H., Paul, P., Kumar, N., Baxi, S., Das, D.P., 2014a. J. Colloid Interface Sci. 430, 221–228.
Gupta, V.K., Atar, N., Yola, M.L., Üstündağ, Z., Uzun, L., 2014b. Water Res. 48, 210–217.
Gupta, V.K., Ganjali, M.R., Norouzi, P., Khani, H., Nayak, A., Agarwal, S., 2011. Crit. Rev. Anal. Chem. 41, 282–313.
Gupta, V.K., Kumar, P., 1999. Anal. Chim. Acta 389, 205–212.
Gupta, V.K., Kumar, S., Singh, R., Singh, L.P., Shoora, S.K., Sethi, B., 2014c. J. Mol. Liq. 195, 65–68.
Gupta, V.K., Mergu, N., Kumawat, L.K., Singh, A.K., 2015a. Talanta 144, 80–89.
Gupta, V.K., Mergu, N., Kumawat, L.K., Singh, A.K., 2015b. Sens. Actuators, B 207, 216–223.
Gupta, V.K., Sethi, B., Sharma, R.A., Agarwal, S., Bharti, A., 2013. J. Mol. Liq. 177, 114–118.
Gupta, V.K., Singh, L.P., Singh, R., Upadhyay, N., Kaur, S.P., Sethi, B., 2012. J. Mol. Liq. 174, 11–16.
Hou, L., Zhu, C., Wu, X., Chen, G., Tang, D., 2014. Sci. Rev. Chem. Commun. 50, 1441–1443.
Jain, A.K., Gupta, V.K., Sahoo, B.B., Singh, L.P., 1995a. Anal. Proc. 32, 99–101.
Jain, A.K., Gupta, V.K., Singh, L.P., 1995b. Anal. Proc. 32, 263–266.
Karthikeyan, S., Gupta, V.K., Boopathy, R., Titus, A., Sekaran, G., 2012. J. Mol. Liq. 173, 153–163.
Karunakaran, G., Kundu, M., Maduraiveeran, G., Kolesnikov, E., Gorshenkov, M.V., Balasingam, S.K., Kumari, S., Sasidharan, M., Kuznetsov, D., 2018. Microporous Mesoporous Mater. 272, 1–7.
Li, N., Lu, W., Pei, K., Yao, Y., Chen, W., 2014. ACS Appl. Mater. Interfaces 6, 5869–5876.
Liao, Y., Cheng, Z., Zuo, W., Thomas, A., Faul, C.F.J., 2017. ACS Appl. Mater. Interfaces 9, 38390–38400.
Liu, J., Sonshine, D.A., Shervani, S., Hurt, R.H., 2010. ACS Nano 4, 6903–6913.
Liu, M., Pan, L., Piao, H., Sun, H., Huang, X., Peng, C., Liu, Y., 2015. ACS Appl. Mater. Interfaces 7, 26017–26021.
Liu, X., Wang, Y., Chen, P., McCadden, A., Palaniappan, A., Zhang, J., Liedberg, B., 2016. ACS Sens. 1, 1416–1422.
Masson, J.F., Obando, L., Beaudoin, S., Booksh, K., 2004. Talanta 62, 865–870.
Nandhikonda, P., Heagy, M.D., 2011. J. Am. Chem. Soc. 133, 14972–14974.
Pan, Y., Zeng, W., Li, L., Zhang, Y., Dong, Y., Ye, K., Cheng, K., Cao, D., Wang, G., Lucht, B.L., 2018. J. Electro Anal. Chem. 810, 248–254.
Ren, K., Wu, J., Yan, F., Zhang, Y., Ju, H., 2015. Biosens. Bioelectron. 66, 345–349.
Ren, X., Ma, H., Zhang, T., Zhang, Y., Yan, T., Du, B., Wei, Q., 2017a. ACS Appl. Mater. Interfaces 9, 37637–37644.
Ren, X., Zhang, T., Wu, D., Yan, T., Pang, X., Du, B., Lou, W., Wei, Q., 2017b. Biosens. Bioelectron. 94, 694–700.
Sarangadharan, I., Wang, S.-L., Sukesan, R., Chen, P.-c., Dai, T.-Y., Pulikkathodi, A.K., Hsu, C.-P., Chiang, H.-H.K., Liu, L.Y.-M., Wang, Y.-L., 2018. Anal. Chem. 90, 2867–2874.
Schulze, M.W., Sinturel, C., Hillmyer, M.A., 2015. ACS Macro Lett. 4, 1027–1032.
Srivastava, S.K., Gupta, V.K., Jain, S., 1995. Analyst 120, 495–498.
Srivastava, S.K., Gupta, V.K., Jain, S., 1996. Anal. Chem. 68, 1272–1275.
Wan, H., Qin, H., Xiong, Z., Zhang, W., Zou, H., 2013. Nanoscale 5, 10936–10944.
Wang, S., Zhao, Y., Wang, M., Li, H., Saqib, M., Ge, C., Zhang, X., Jin, Y., 2019. Anal. Chem. 91, 3048–3054.
Wang, W., Wang, Y., Li, C., Yan, L., Jiang, M., Ding, Y., 2017. ACS Sustain. Chem. Eng. 5, 4523–4528.
Xuan, S., Wang, F., Lai, J.M.Y., Sham, K.W.Y., Wang, Y.-X.J., Lee, S.-F., Yu, J.C., Cheng, C.H.K., Leung, K.C.-F., 2011. ACS Appl. Mater. Interfaces 3, 237–244.
Yang, Z.-H., Zhuo, Y., Yuan, R., Chai, Y.-Q., 2016. Sens. Actuators, B 227, 212–219.
Yola, M.L., Gupta, V.K., Eren, T., Şen, A.E., Atar, N., 2014. Electrochim. Acta 120, 204–211.
Zhang, Q., Huang, Y., Jiang, B., Hu, Y., Xie, J., Gao, X., Jia, B., Shen, H., Zhang, W., Yang, P., 2018a. Anal. Chem. 90, 7357–7363.

Zhang, T., Ma, N., Ali, A., Wei, Q., Wu, D., Ren, X., 2018b. Biosens. Bioelectron. 119, 176–181.
Zhang, T., Xing, B., Han, Q., Lei, Y., Wu, D., Ren, X., Wei, Q., 2018c. Anal. Chim. Acta 1032, 114–121.
Zhang, Z., Balogh, D., Wang, F., Willner, I., 2013. J. Am. Chem. Soc. 135, 1934–1940.
Zheng, Q., Zhang, H., Shi, B., Xue, X., Liu, Z., Jin, Y., Ma, Y., Zou, Y., Wang, X., An, Z., Tang, W., Zhang, W., Yang, F., Liu, Y., Lang, X., Xu, Z., Li, Z., Wang, Z.L., 2016. ACS Nano 10, 6510–6518.
Zhu, M., Ye, R., Jin, K., Lazouski, N., Manthiram, K., 2018. ACS Energy Lett 3, 1381–1386.
Zou, C., Li, Q., Hua, Y., Zhou, B., Duan, J., Jin, W., 2017. ACS Appl. Mater. Interfaces 9, 29093–29100.

Ning Ma studies in school of chemistry and chemical engineering, University of Jinan as postgraduate student.

Tong Zhang studies in school of chemistry and chemical engineering, University of Jinan as postgraduate student.

Xuan Kuang obtained her Ph.D. in Analytical Chemistry in 2015. Her research interests focus on metal organic materials and the application of nanomaterials to electrochemical sensors, synthesis and fundamental electrochemical studies of energy storage devices and synthetic nanomotors.

Dan Wu a professor and received the D.S. degree from Shandong University in 2005. She dedicates to the surfactant and biological macromolecules interaction. And now she also studies the role of surfactant in electrochemical immunosensor.

Qin Wei a professor and DSc, has devoted herself to analytical teaching and scientific research. Her main research interests are the determination of protein and nucleic acid by photometry and the electrochemical immunosensor preparation. She has published over one hundred articles on analysis, immunosensor and applied successfully for many research projects, such as Biomaterials, Adv. Funct. Mater., Biosens. Bioelectron., Sens. Actuators B: Chem., Talanta.